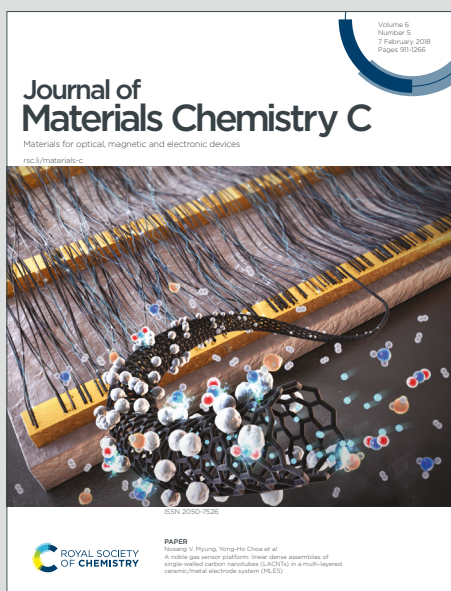


Journal of Materials Chemistry C

Materials for optical, magnetic and electronic devices

Accepted Manuscript

This article can be cited before page numbers have been issued, to do this please use: Y. Zeng, P. Tan, T. Han, K. Liu, P. Mu, B. Yue, H. Gou, Y. Wang, D. X. Yao, W. Sang, N. Wang and M. Li, *J. Mater. Chem. C*, 2025, DOI: 10.1039/D5TC01779C.



This is an Accepted Manuscript, which has been through the Royal Society of Chemistry peer review process and has been accepted for publication.

Accepted Manuscripts are published online shortly after acceptance, before technical editing, formatting and proof reading. Using this free service, authors can make their results available to the community, in citable form, before we publish the edited article. We will replace this Accepted Manuscript with the edited and formatted Advance Article as soon as it is available.

You can find more information about Accepted Manuscripts in the [Information for Authors](#).

Please note that technical editing may introduce minor changes to the text and/or graphics, which may alter content. The journal's standard [Terms & Conditions](#) and the [Ethical guidelines](#) still apply. In no event shall the Royal Society of Chemistry be held responsible for any errors or omissions in this Accepted Manuscript or any consequences arising from the use of any information it contains.

Cite this: DOI: 00.0000/xxxxxxxxxx

A computational and Raman spectroscopic study of successive phase transitions in Co_3TeO_6 under high pressure and high temperature[†]Yijie Zeng,^{a‡} Pengfei Tan,^{b‡} Tao Han,^b Ke Liu,^c Peiyang Mu,^c Binbin Yue,^c Huiyang Gou,^c Yonggang Wang,^d Dao-Xin Yao,^{*e} Weidong Sang,^f Na Wang,^f and Man-Rong Li^{*f}Received Date
Accepted Date

DOI: 00.0000/xxxxxxxxxx

Co_3TeO_6 was previously found to transform from nonpolar (point group C_{2h}) to polar (C_3) antiferromagnet (AFM) at 5 GPa and 1023 K, of which the transition pressure was predicted by first-principles calculations assuming ferromagnetic (FM) ground states. Here we report a computational contrast experiment on the transition pressure in Co_3TeO_6 , followed by verification experiment. The $C2/c$ to $R3$ transition is reproduced by both FM (4.7 GPa) and AFM (4.5 GPa) calculations. A further phase transition from $R3$ to $P2_1/n$ is predicted to occur at 16.2 (FM) or 19.2 GPa (AFM). To avoid cell deformation due to reduced symmetry in AFM calculation, FM-optimized unit cell is used. This strategy is inspired from calculations on Mn_3TeO_6 , whose magnetic structure preserves the paramagnetic point group and a direct AFM calculation is feasible. Refinement of ex situ powder X-ray diffraction data of Co_3TeO_6 polymorphs prepared under ambient pressure, 5 GPa, and 20 GPa (and high temperature, then quenched and decompressed to ambient pressure for the latter two) show $C2/c$, $R3$ and phase coexistence of $R3$ (72%) and $P2_1/n$ (28%), respectively. Pressure-dependent Raman spectroscopy on polymorphs with $C2/c$ and $R3$ phases at room temperature show no hints of phase transition. Our preliminary diffraction and spectroscopy results indicate that kinetic effects in phase transition cannot be ignored, and serve as a foundation for future in situ investigations.

1 Introduction

Co_3TeO_6 is a double perovskites (DPv, $A_2BB'O_6$) with small magnetic cations (e.g. Mn^{2+} , Co^{2+} , Ni^{2+})^{1–6} on A and B -sites. Due to the low structural tolerance factor t^7 , it adopts highly distorted perovskite-related structure at ambient pressure (AP)⁸, the β - Li_3VF_6 ($C2/c$) structure⁹. It transforms to polar polymorphs when prepared under high-pressure (HP) and high-temperature (HT)⁴, and combined with complex antiferromagnetic (AFM) magnetic structures^{5,10,10–12}, magnetoelectric coupling can occur⁴. There are conflicting conclusions on whether further phase transition exists in Co_3TeO_6 as pressure increases: The calculations by Y.

Han *et al.*⁴ show that there is no further transition up to 25 GPa, except the $C2/c$ to $R3$ transition at 5 GPa. E. Solana-Madruga *et al.*¹³ show that 14.5% of Co_3TeO_6 is in $P2_1/n$ when prepared at 15 GPa, with two AFM structures ($k = [\frac{1}{2}, 0, \frac{1}{2}]$ and $k_0 = [0, 0, 0]$), suggesting another phase transition from $R3$ to $P2_1/n$ is possible at higher pressure.

The experimental investigation of HP and HT synthesis is generally a trial-and-error process, where both the HP phase and transition pressure are unknown¹⁴. Recent works show it is possible to determine the HP phase by data mining and the transition pressure by comparing the enthalpies of HP phases with that of AP polymorph¹⁵. Although this is a straightforward work for nonmagnetic DPv, one encounters extra complexity in magnetic DPv, if the magnetic structures (mostly AFM) are to be considered. Previous works on magnetic DPv e.g. Mn_3TeO_6 ^{16,17} and Co_3TeO_6 ⁴, tackle this problem by assuming ferromagnetic (FM) ground states for the involved structures^{18,19}. The FM method has the advantage to avoid considering the complex AFM magnetic structure, which can be incommensurate with the paramagnetic unit cell^{3,4,9,20–27}. Moreover, the FM unit cell is the same as the paramagnetic one, thus avoiding the problem of cell deformation during constant-volume optimization. Even so, it would be desirable to estimate the error in transition pressure caused by assuming FM state. Also, the calculated electronic property is

^a School of Science, Hangzhou Dianzi University, Hangzhou 310018, China.^b Key Laboratory of Bioinorganic and Synthetic Chemistry of Ministry of Education, School of Chemistry, Sun Yat-Sen University, Guangzhou 510006, China.^c Center for High Pressure Science and Technology Advanced Research (HPSTAR), Beijing 100193, China.^d School of Materials Science and Engineering, Peking University, Beijing 100871, China.^e State Key Laboratory of Optoelectronic Materials and Technologies, Guangdong Provincial Key Laboratory of Magnetoelectric Physics and Devices, School of Physics, Sun Yat-sen University, Guangzhou 510275, China. E-mail: yaodaoo@mail.sysu.edu.cn^f School of Chemistry and Chemical Engineering, Hainan University, Haikou 570228, China. E-mail: limanrong@mail.sysu.edu.cn[†] Supplementary Information available: [details of any supplementary information available should be included here]. See DOI: 00.0000/00000000.[‡] These authors contributed equally to this work.

correct only if the AFM ground state is considered.

Here we reconsider the polymorphy evolution of Co_3TeO_6 under HP (and HT). By performing a thorough calculation assuming both FM and AFM states, we show that the predicted transition pressure by FM method is very close to the one predicted by AFM method, whereas the computational effort is much reduced. To perform a direct constant-volume AFM calculation, the AFM unit cell should not break the paramagnetic point group symmetry. The AFM structures of both AP and HP phases of Co_3TeO_6 do not meet this requirement, while Mn_3TeO_6 does. The magnetic structure of HP phase Mn_3TeO_6 is P_C2_1/n^{17} (14.84 in BNS notation), which preserves the paramagnetic point group symmetry. The results on Mn_3TeO_6 show that the optimized unit cells by both methods have almost the same lattice parameters, suggesting that it is reasonable to do AFM calculation in two-steps: first optimizing the cell assuming FM state, then calculating total energy assuming AFM state. This two-step AFM method is then used for Co_3TeO_6 , the $C2/c$ to $R3$ transition is reproduced by both FM (4.7 GPa) and AFM (4.5 GPa) calculations, and a further $R3$ to $P2_1/n$ phase transition is found at 16.2 GPa (or 19.2 GPa, AFM).

Moreover, our preliminary diffraction and spectroscopy results show the $R3$ to $P2_1/n$ transition is partially realized. Powder X-ray diffraction (PXD) on polymorphs prepared under 20 GPa 1473 K starting from samples in $R3$ phase, then quenched to room temperature (RT) and decompressed to AP, show phase coexistence of $R3$ (28%) and $P2_1/n$ (72%). The new phase is also supported by appearance of new peaks in Raman spectra of samples prepared under 20 GPa, compared with polymorphs prepared at AP ($C2/c$) and 5 GPa ($R3$). Pressure-dependent Raman spectra on samples in both $C2/c$ and $R3$ phases at RT show no hints of phase transition. The phase coexistence is attributed to a high energy barrier in kinetic process of the $R3$ to $P2_1/n$ transition.

2 Methods

2.1 Computational methods

The first-principles calculations are performed using Vienna *ab initio* package (VASP)²⁹, with PAW potentials^{30,31}. The cutoff energy is 700 eV, and a Monkhorst-Pack grid of $9 \times 9 \times 9$ ($7 \times 9 \times 7$ for AFM configuration of $P2_1/n$) for Mn_3TeO_6 and $9 \times 9 \times 9$ ($7 \times 7 \times 7$ for AFM), $5 \times 7 \times 5$ and $9 \times 9 \times 9$ for Co_3TeO_6 in $R3$, $C2/c$ and $P2_1/n$ are used for integration in reciprocal space, respectively. The structures are optimized under constraint of constant volume and preserving the given magnetic point group symmetry. All the atoms are allowed to relax until the forces are converged to be less than 0.01 eV/Å. The LDA+U method introduced by Dudarev *et al.*³² is used, with $U = 3.0$ eV for Mn and Co. SOC is not considered.

2.2 Sample preparation

The AP Co_3TeO_6 phase was synthesized by solid-state reaction method using stoichiometric mixture of CoO (99.9%, Aladdin) and TeO_2 (99.99%, Alfa Aesar) as the starting components. The reagents were weighed, mixed and ground well in an agate mortar before being successively calcined (heating rate of 300 K/h) at 773 K for 24 h, 1023 K for 24 h, and 1173 K for 24 h with several

intermediate grinding. After each calcination, the powder was natural cooling down to RT. The identification of phase purity and crystal structure were conducted by powder X-ray diffraction (PXD, SmartLab SE diffractometer, Rigaku, Japan) instrument with Cu $K\alpha$ tube ($\lambda = 1.5418$ Å at 40 kV and 30 mA) between 10 and 120° (step size 0.02°, 10 s per step), as shown in Fig.S1(a) in Supplemental informations (SI). Rietveld refinements were performed using TOPAS Academic V6 software package³³. The refined crystallographic information is listed in Table S1.

To synthesize the $R3$ phase, the as-prepared AP- Co_3TeO_6 was loaded into Pt capsules and treated at 5 GPa and 1073 K for 30 min in a Walker-type multi-anvil HP apparatus. Finally, the sample was quenched to RT and followed by a slow pressure decompression. The crystal structure was determined by using synchrotron powder diffraction (SPXD). SPXD data was collected at ambient condition on beamline BL14B ($\lambda = 0.6900$ Å) at the Shanghai Synchrotron Radiation Facility (SSRF), as shown in Fig.S1(b). The refined crystallographic information is listed in Table S2.

To synthesize the predicted $P2_1/n$ phase, the as-prepared $R3$ sample was loaded into Pt capsules and treated at 20 GPa and 1473 K for 30 min in a Walker-type multi-anvil high-pressure apparatus. Then the sample was also quenched to RT and followed by a slow pressure decompression.

2.3 In Situ pressure-dependent Raman spectroscopy

In situ HP Raman spectra were recorded on a Renishaw Raman microscope using a 532 nm laser (with laser power about 30 mW) up to 31.4 GPa at RT. The system was calibrated by the Raman signal of Si, and the spectra were collected in the range of 40 to 1250 cm^{-1} . A symmetric diamond anvil cell (DAC) with type Iia diamonds polished to a diameter of 400 μm was used to generate the HP. Steel gaskets were pre-indented to 40 μm thick, and 180 μm holes were drilled to serve as the sample chambers. The pre-compressed samples were loaded, together with ruby balls, into the sample chamber, and pressure was calibrated using the ruby fluorescence peak. All the in situ HP measurements use silicone oil as the pressure transfer medium (PTM).

3 Results and Discussion

3.1 Computational Results

Mn_3TeO_6 .— Mn_3TeO_6 crystallizes in Mg_3TeO_6 ($R\bar{3}$) structure³⁴ at AP, with magnetic propagation vector $k = [0, 0, 0.4302]$ below 23 K, which is a helical spiral magnetic structure incommensurate with the crystal structure^{25,35}. Under 5 GPa¹⁶ (or 8 GPa¹⁷) and 1173 K, it transforms into $P2_1/n$ double perovskite structure, with $k = [\frac{1}{2}0\frac{1}{2}]$ below 36 K¹⁷ and magnetic moments 4.8 and 3.8 μ_B for Mn_A and Mn_B , respectively. The lattice parameters and atomic coordinates reported by experiment^{16,17} are listed in Table S4.

If we assume FM states, the spin groups are $[E||C_{3i}]$ and $[E||C_{2h}]$ for $R\bar{3}$ and $P2_1/n$, respectively, which preserve the paramagnetic point group symmetries, and the crystallographic unit cell can be used, as shown in Fig.1. If AFM states are assumed, care should be taken when dealing with $R\bar{3}$: the experimental magnetic structure is incommensurate, an exact first-principles description of the magnetic unit cell is beyond current calculation capabilities.

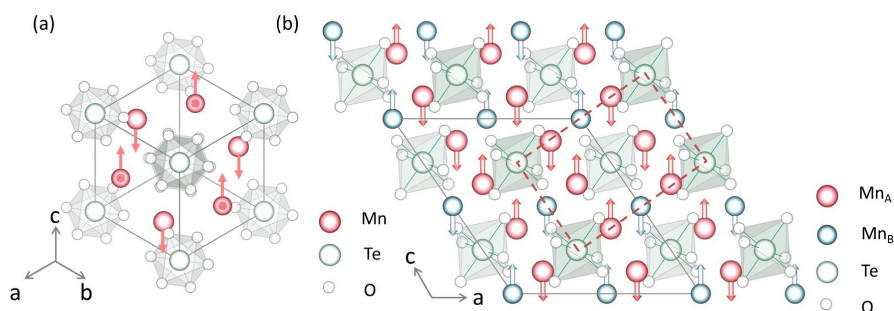


Fig. 1 The AFM unit cells of Mn_3TeO_6 (a) at AP ($R\bar{3}$) and (b) HP ($P2_1/n$), the upward (downward) arrows on Mn atoms mean spin-up (spin-down). The crystallographic unit cell is the same as the AFM unit cell for $R\bar{3}$, and is halved for $P2_1/n$, as shown by the dashed parallelogram.

Instead, we use a commensurate AFM structure with $k = [0, 0, 0]$, by dividing the Mn (18f) atoms into two groups with opposite spins. Each group is connected to the other by inversion symmetry and S_6 , and atoms within each group are connected by C_3 (Fig.1(a)). While for the AFM state of $P2_1/n$, the experimental magnetic structure¹⁷ $P2_1/n$ is used, where the magnetic unit cell is doubled (Fig.1(b)). Under these AFM structures the corresponding spin groups are $[E||C_3] + [C_2||IC_3]$ and $[E||C_{2h}]$, and a cell optimization preserving the symmetry of given crystal system is feasible³⁶.

The calculated $E - V$ curves are shown in Fig.2(a). The AFM state has lower energy than FM one at the same volume (for the same polymorph), indicating that AFM is the ground state, consistent with experiment. However, the energy difference is tiny compared to that due to volume collapse, e.g., for $R\bar{3}$ the energy difference between FM and AFM states varies from 0.074 to 0.800 eV in the considered volume range, while that due to volume collapse is 15 eV. This can be understood since energy of the magnetic interaction is of *meV* order. The deduced $H - P$ relations show almost the same shape, and the predicted transition pressures are 8.0 and 6.9 GPa for FM and AFM states, respectively, somehow larger than the experimental value of 5 GPa. The result of AFM configuration is closer to the experimental value, at the cost of increased computational time, due to that the AFM unit cell of $P2_1/n$ is doubled.

The lattice parameters for $R\bar{3}$ and $P2_1/n$ at the sampled volumes are shown in Fig.3 (typical atomic positions are listed in Table S4), from which it is obvious that the lattice parameters optimized under FM and AFM states are almost the same at a given volume in the considered range, with the maximum difference being $\Delta a_H = 0.03$, $\Delta c_H = 0.08$ angstroms for $R\bar{3}$ and $\Delta a = 0.04$, $\Delta b = 0.03$, $\Delta c = 0.01$ angstroms, $\Delta\beta = 0.2^\circ$ for $P2_1/n$. Such tiny difference means the global minimums of energy landscapes for FM and AFM states are located at nearly the same configuration, or the cell shapes of FM and AFM states are nearly the same.

The above feature suggests that it is reasonable to calculate the cell shape (or lattice parameters) by assuming FM state, and then recalculate the total energy using the correct AFM state, with the FM-determined cell. The total energy should be the same (within a given error range) as that calculated by relaxing both the cell shape and atomic positions assuming AFM state. We recalculate the $E - V$ curves by this “two-step” method, the results of which

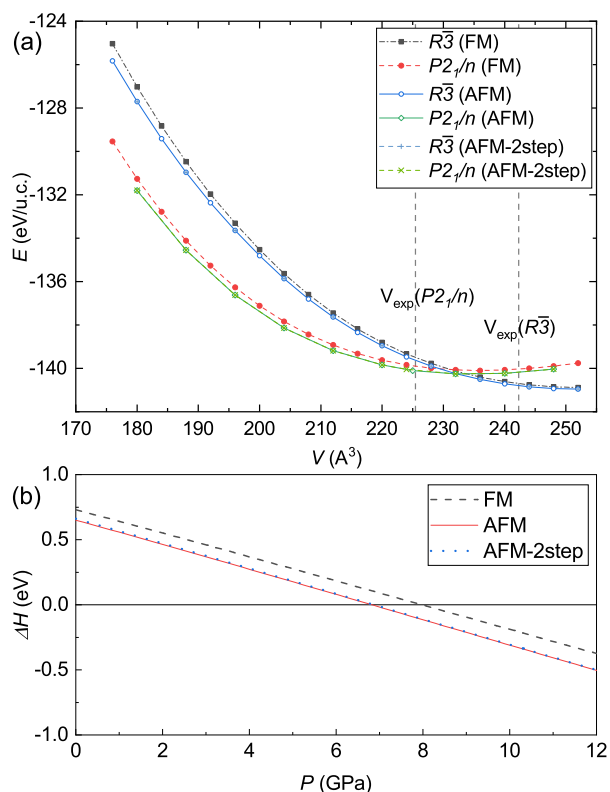


Fig. 2 (a) The $E - V$ curves of Mn_3TeO_6 in $P2_1/n$ and $R\bar{3}$. (b) the $\Delta H - P$ relations assuming FM, AFM and AFM with two-step method, respectively, $\Delta H = H(P2_1/n) - H(R\bar{3})$.

are shown in Fig.2(a). It's clear that the $E - V$ curves nearly overlap those assuming AFM state, with maximum difference in E being less than 2 meV/u.c., which is a rather good result. It is then expected that the $H - P$ relation, and the predicted transition pressure by this method also agree well with those assuming AFM state and optimized directly (Fig.2(b)).

Note that the AFM state used for $R\bar{3}$ is not the real ground state. If the incommensurate AFM state is used, the $E - V$ curve for $R\bar{3}$ will move downward slightly, and the predicted transition pressure will be a bit larger than 6.9 GPa. The difference between the predicted and experimental transition pressures may come from the neglecting of zero-point energies of $R\bar{3}$ and $P2_1/n$ and temperature effect, or the insufficient consideration of correlation

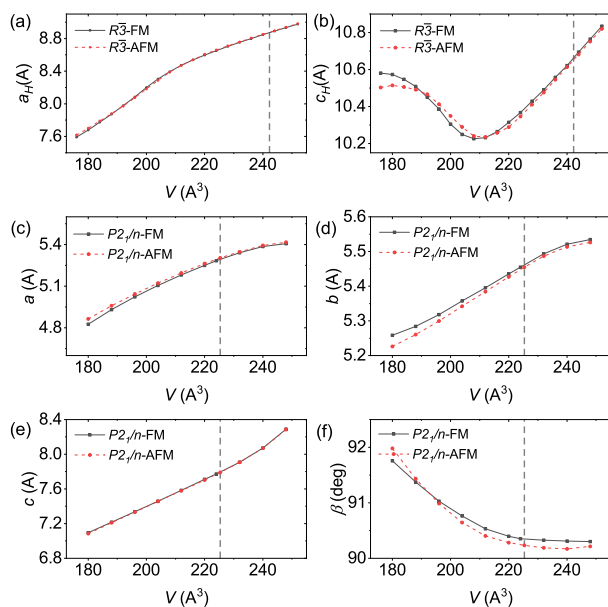


Fig. 3 The lattice parameters of Mn_3TeO_6 at sampled volumes. (a) a_H , (b) c_H for $R\bar{3}$ and (c) a , (d) b , (e) c , (f) β for $P2_1/n$, respectively. The vertical dashed lines represent the experimental volumes of unit cell.

by LDA+U method, which are beyond the scope of the present work.

Co_3TeO_6 .—We then proceed to consider the phase transition of Co_3TeO_6 , which crystallizes in $C2/c$ at AP³⁷, with five Co^{2+} sublattices in the unit cell. The magnetic structure is complex⁹, with incommensurate $k = [0, 0.485, 0.055]$ below 26 K. It transforms to $k = [0, 0, 0]$ below 21.1 K, and further to $k = [0, 0.5, 0.25]$ below 17.4 K. The results of neutron diffraction, magnetic susceptibility and dielectric parameters establish it is a type-II multiferroics³⁸. It transforms into polar Ni_3TeO_6 structure³⁹ ($R3$) at 5 GPa and 1023 K⁴ (or 6.5 GPa and 1073 K⁴⁰), with a complex helix magnetic structure below 58 K^{4,13}.

The AFM states considered are shown in Fig.4(a) for $C2/c$ (with $k = [0, 0, 0]$) and (b,c) for $R3$, respectively. For $P2_1/n$ the k_0 magnetic structure found by E. Solana-Madruga *et al.*¹³ is considered. For $R3$, four AFM structures shown in Fig.4(c), rather than the helix magnetic structure, are considered. To decide which one is the “ground state”, we fix the volume of the unit cell to the reported experimental value (214.92 \AA^3)⁴, and relax the atomic coordinates at sampled lattice parameters. The results are shown in Fig.4(d), from which it is clear that the type-I AFM magnetic structure is most stable, which is the same as in Ni_3TeO_6 ³⁹. This behaviour is unchanged when the volume is further compressed, as verified by our calculation for $V = 210 \text{ \AA}^3$ (see Fig.S4). The energy minimums for all considered magnetic structures (including FM structure) are located at nearly the same point in the parameter space formed by lattice parameters⁴¹, and the cell shapes of AFM and FM states can be regarded the same. This is supported by the structural evolution measurement between 5 and 90 K⁴, where the maximum changes of a and c are less than 0.01 \AA .

For $C2/c$ it is computation-demanding, though not impossible, to calculate the energy surface in parameter space with three free parameters at a given volume ($a \neq b \neq c$, with $\beta \neq 90^\circ$). We hy-

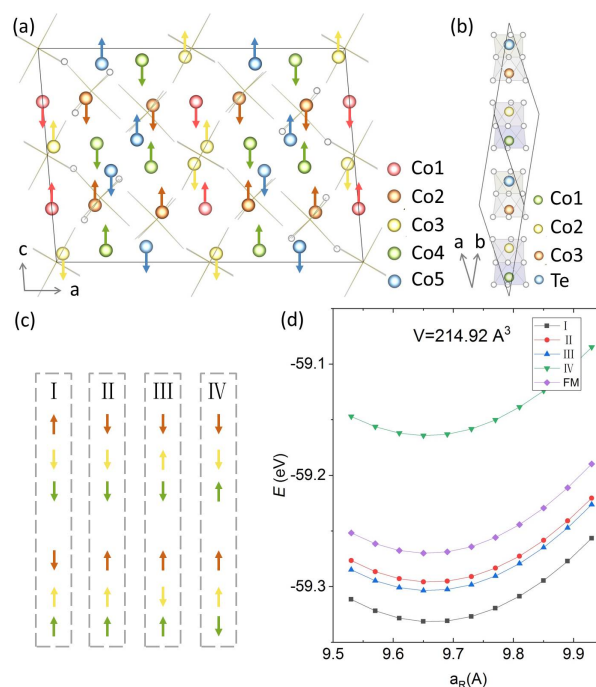


Fig. 4 The AFM unit cells of Co_3TeO_6 (a) at AP ($C2/c$) and (b) HP ($R3$). The Te-O octahedrons are shown in wireframes in (a) to highlight the Co sublattices. The actual unit cell of $C2/c$ is half of that shown in (a). (d) The $E - a_R$ curves for $R3$ at $V = 214.92 \text{ \AA}^3$ with different magnetic structures, as shown in (c).

pothesize the cell shapes of AFM and FM states are also the same for $C2/c$, which is supported by experimental fact that the maximum change of lattice parameters⁹ between 1.6 and 50 K is below 0.02 \AA , while the magnetic structure transforms successively in this temperature range.

The calculated $E - V$ curves are shown in Fig.5(a). The AFM states have lower energy than FM states at all sampled volumes, as expected. The deduced $H - P$ curves for FM and AFM states are shown in Fig.5(b). The $C2/c$ to $R3$ transition is reproduced by both assumptions, with predicted transition pressure 4.7 (4.5) GPa for FM and AFM states, respectively. Furthermore, both FM and AFM (two-step method) results give clear evidence of phase transition from $R3$ to $P2_1/n$, at 16.2 and 19.2 GPa, respectively, close to and a little higher than the experimental value 15 GPa under which portion of Co_3TeO_6 crystallizes in $P2_1/n$ ¹³. The 3 GPa difference is caused by the energy difference between AFM and FM states of $P2_1/n$ being smaller than that of $R3$, which might originate from reduced exchange coupling between Co_A and Co_B in $P2_1/n$ compared to that between Co_1 and Co_2 in $R3$ (see Fig.S2). Besides, we find the $k = [\frac{1}{2}, 0, \frac{1}{2}]$ state is higher in energy than $k_0 = [0, 0, 0]$, indicating that the ground state magnetic structure of Co_3TeO_6 in $P2_1/n$ is different from that of Mn_3TeO_6 in $P2_1/n$.

3.2 Experimental Results

Pressure-dependent Raman spectra at RT.—To study the possible phase transition near 20 GPa, we first carry out pressure-dependent Raman spectroscopy at RT, using AP phase samples ($C2/c$) and $R3$ phase samples (synthesized under 5 GPa and 1073

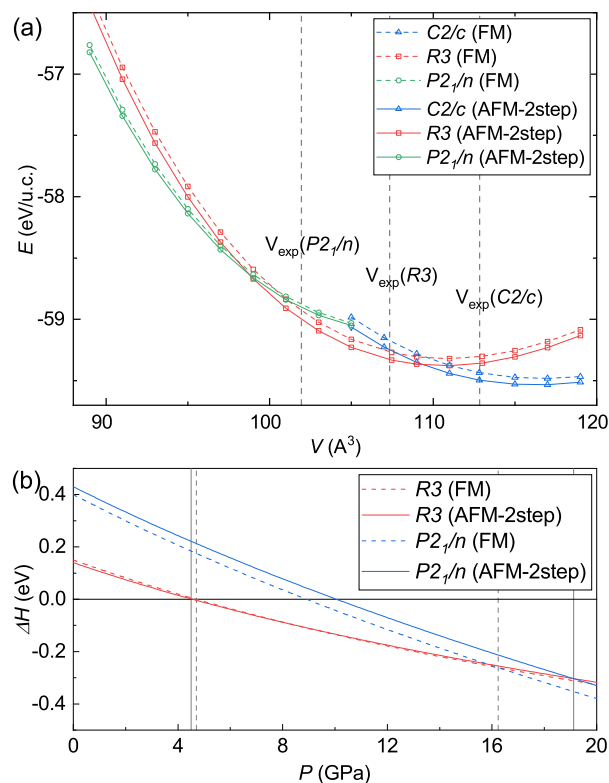


Fig. 5 (a) The $E - V$ curves of Co_3TeO_6 in $C2/c$, $R3$ and $P2_1/n$. (b) the $\Delta H - P$ relations assuming FM state, and AFM state with two-step method, respectively. The enthalpy of $C2/c$ is taken as reference. The dashed (solid) vertical lines indicate the predicted transition pressures assuming FM state (AFM state with two-step method).

K, then quenched to RT and decompressed to AP), respectively. The results are shown in Fig.6(a) and (b). The Raman spectra of AP phase samples do not show clear changes around 5 GPa, although the peak near 730 cm^{-1} blue shifts as pressure increases (Fig.S5). The Raman spectra of $R3$ phase samples is clearly different from that of AP phase samples (for example, the AP phase at 1.8 GPa and the $R3$ phase at 1.3 GPa): there are no subpeaks around the main peak at about 700 cm^{-1} , there is no peak near 510 cm^{-1} , and the whole spectra show the same peak patterns up to 26.6 GPa. These features indicate that both AP phase and $R3$ phase remain unchanged at RT, even though the pressure has reached or is larger than the transition pressure. This is related to the fact that the atomic arrangements are so different for the three phases (for $C2/c$ Co sit in octahedron and tetrahedron polyhedra, which have corner, edge and face-sharing connections⁹, for $R3$ only octahedron polyhedra exists, for $P2_1/n$ the face-sharing connection disappears), although pressure had reached the critical point, HT is needed so that the cations can vibrate in large amplitudes to break the bonds and rearrange to form the new phase. For phase transitions involving slight change of atomic arrangements, HP alone can induce phase transition at RT, e.g. in MnTa_2O_6 ⁴² or FePX_3 ($X = \text{S}, \text{Se}$)⁴³.

Evidence of new phase.— After establishing the role of HT, we then prepared samples under 20 GPa and 1473 K, starting from as-prepared $R3$ phase sample. After being quenched and decom-

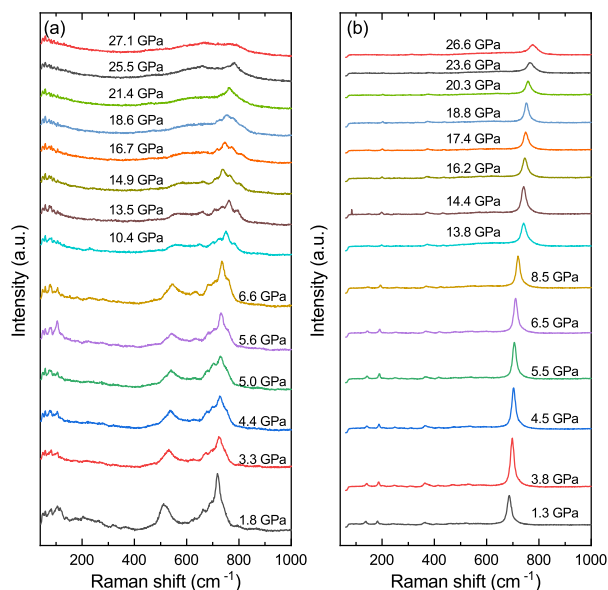


Fig. 6 Raman spectra of Co_3TeO_6 in AP phase ($C2/c$) and (b) $R3$ phase, respectively, collected under different pressures and RT.

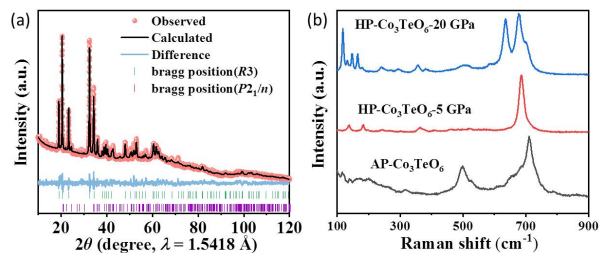


Fig. 7 (a) Refinements of the PXD data of the synthesized Co_3TeO_6 samples were obtained at 20 GPa and 1473 K. (b) Raman spectra of the Co_3TeO_6 samples in different polymorphs collected at RT and AP.

pressed to AP, the phase and crystal structure of the sample was determined by PXD. As shown in Fig.7(a), some extra diffraction peaks can be observed after the high pressure treatment (compared to Fig.S1), indicating the occurrence of phase transition. Rietveld fitting of PXD data show phase coexistence refined to 72% $R3$ and 28% $P2_1/n$ (Table S3). Due to the limitation of our equipment, we can not synthesize pure $P2_1/n$ phase under higher pressure or temperature. Raman spectroscopy were then performed on the sample to identify the change of crystal structure. As evidenced in Fig.7(b), there are two main peaks around 700 cm^{-1} , and a new peak at about 120 cm^{-1} appears, which are distinct from both $C2/c$ and $R3$ phases, indicating that the sample might adopt a new phase.

Possible causes of phase coexistence.— The samples prepared under 20 GPa and 1473 K show phase coexistence when quenched and decompressed. One possibility is the samples are in $P2_1/n$ phase in the sample chamber at 20 GPa, but recover partially to $R3$ when decompressed, similar to ScFeO_3 ⁴⁴, which turns from orthorhombic perovskite at 15 GPa to LiNbO_3 -type structure when decompressed to AP at RT and vice versa. However, if the $R3$ - $P2_1/n$ transition is reversible, and note the fact that decompression takes place at RT, this possibility can be excluded from our

pressure-dependent Raman spectra on *R3* samples at RT, since no phase transition occurred when the *R3* samples were compressed. In situ HP-HT SPXRD or neutron powder diffraction measurements can clarify this point. Another possibility is the synthesis temperature is not high enough or uniformly distributed, preventing the completion of transformation. It is also possible that partial back transformation occurs during quenching. Both are related to considerable energy barrier height of kinetic process in phase transition.

Conclusions

In conclusion, we performed a contrast experiment to clarify the role of magnetic structures on predicted transition pressures of Co_3TeO_6 under HP (and HT). As lattice parameters are insensitive to magnetic structures compared to HP, it is practically a good approximation to assume FM states for all polymorphs and ignore the generally complex AFM structures, without affecting much the predicted transition pressure. This treatment may be extended to other DPv with AFM ground states (see the variation of lattice parameters with temperature in Table S5). Our ex situ PXD data on samples prepared under 20 GPa and 1473 K (then quenched to RT and slowly decompressed to AP) suggests a phase coexistence of *R3* (72%) and $P2_1/n$ (28%). Raman spectra of these samples show new peaks compared to those of *C2/c* and *R3* phases, supporting the appearance of a new phase. Moreover, pressure-dependent Raman spectra on *C2/c* and *R3* samples at RT show no hints of phase transition. The phase coexistence suggests that there might be a high energy barrier associated with the kinetic process of the *R3* to $P2_1/n$ transition, which is not captured by our "zero-temperature" calculation where the motions of ions are ignored. Our preliminary and limited experimental results call for and serve as a foundation for future in situ investigations.

Author contributions

D.Y. and M.L. devised the idea and experiment, Y.Z. performed the calculations, P.T. and T.H. grew the polymorphs, T.H., K.L., P.M., B.Y., H.G. and Y.W. performed the high pressure Raman spectroscopic experiment, W.S. and N.W. analyzed the Raman result. All the authors contributed to the writing of the manuscript.

Conflicts of interest

There are no conflicts to declare.

Data availability

The data supporting this article have been included as part of the Supplementary Information.

Acknowledgements

Y.Z. would like to thank M.-H. Zhao, S. Zhao, W. Su and R. Arita for helpful discussions. The authors thank beamlines BL14B1 (SSRF) for providing the beam time and assistance. This work is supported by the National Science Foundation of China (NSFC-22090041, NSFC-11974432, NSFC-92165204), NKRDP-2022YFA1402802, NKRDP-2018YFA0306001, Zhejiang Provincial Natural Science Foundation (Grant No.LQ21A040010), the Program for Guangdong Introduc-

ing Innovative and Entrepreneurial Teams (2017ZT07C069), the Guangdong Basic and Applied Basic Research Foundation (Grant No.2022B1515120014), Leading Talent Program of Guangdong Special Projects (201626003), Shenzhen International Quantum Academy (Grant No.SIQA202102), the Startup Fund at Hangzhou Dian University (No.KYS075623004) and China Scholarship Council (No.202208330151).

Notes and references

- 1 M. H. Zhao, W. Wang, Y. Han, X. Xu, Z. Sheng, Y. Wang, M. Wu, C. P. Grams, J. Hemberger, D. Walker, M. Greenblatt and M. R. Li, *Inorg Chem*, 2019, **58**, 1599–1606.
- 2 E. Solana-Madruga, A. J. Dos Santos Garca, A. M. Arvalo-Lspez, D. vila Brande, C. Ritter, J. P. Attfield and R. Saez-Puche, *Dalton Transactions*, 2015, **44**, 20441–20448.
- 3 M. R. Li, E. E. McCabe, P. W. Stephens, M. Croft, L. Collins, S. V. Kalinin, Z. Deng, M. Retuerto, A. Sen Gupta, H. Padmanabhan, V. Gopalan, C. P. Grams, J. Hemberger, F. Orlandi, P. Manuel, W. M. Li, C. Q. Jin, D. Walker and M. Greenblatt, *Nat Commun*, 2017, **8**, 2037.
- 4 Y. Han, M. Wu, C. Gui, C. Zhu, Z. Sun, M.-H. Zhao, A. A. Savina, A. M. Abakumov, B. Wang, F. Huang, L. He, J. Chen, Q. Huang, M. Croft, S. Ehrlich, S. Khalid, Z. Deng, C. Jin, C. P. Grams, J. Hemberger, X. Wang, J. Hong, U. Adem, M. Ye, S. Dong and M.-R. Li, *npj Quantum Materials*, 2020, **5**, 92.
- 5 Y. S. Oh, S. Artyukhin, J. J. Yang, V. Zapf, J. W. Kim, D. Vanderbilt and S. W. Cheong, *Nat Commun*, 2014, **5**, 3201.
- 6 M. R. Li, P. W. Stephens, M. Retuerto, T. Sarkar, C. P. Grams, J. Hemberger, M. C. Croft, D. Walker and M. Greenblatt, *J Am Chem Soc*, 2014, **136**, 8508–11.
- 7 C. J. Bartel, C. Sutton, B. R. Goldsmith, R. H. Ouyang, C. B. Musgrave, L. M. Ghiringhelli and M. Scheffler, *Science Advances*, 2019, **5**, eaav0693.
- 8 E. Solana-Madruga and A. M. Arvalo-Lspez, *Journal of Solid State Chemistry*, 2022, **315**, 123470.
- 9 S. A. Ivanov, R. Tellgren, C. Ritter, P. Nordblad, R. Mathieu, G. Andr, N. V. Golubko, E. D. Politova and M. Weil, *Materials Research Bulletin*, 2012, **47**, 63–72.
- 10 G.-H. Cai, M. Greenblatt and M.-R. Li, *Chemistry of Materials*, 2017, **29**, 5447–5457.
- 11 Y. Tokura, S. Seki and N. Nagaosa, *Rep Prog Phys*, 2014, **77**, 076501.
- 12 M. Ye and D. Vanderbilt, *Physical Review B*, 2016, **93**, 134303.
- 13 E. Solana-Madruga, C. Aguilar-Maldonado, C. Ritter, M. Huve, O. Mentre, J. P. Attfield and A. M. Arevalo-Lopez, *Chem Commun (Camb)*, 2021, **57**, 2511–2514.
- 14 Y. Inaguma, A. Aimi, Y. Shirako, D. Sakurai, D. Mori, H. Kojitani, M. Akaogi and M. Nakayama, *J Am Chem Soc*, 2014, **136**, 2748–56.
- 15 M.-H. Zhao, C. Zhu, Z. Sun, T. Xia, Y. Han, Y. Zeng, Z. Gao, Y. Gong, X. Wang, J. Hong, W.-X. Zhang, Y. Wang, D.-X. Yao and M.-R. Li, *Chemistry of Materials*, 2021, **34**, 186–196.
- 16 H.-P. Su, S.-F. Li, Y. Han, M.-X. Wu, C. Gui, Y. Chang, M. Croft,

- S. Ehrlich, S. Khalid, U. Adem, S. Dong, Y. Sun, F. Huang and M.-R. Li, *Journal of Materials Chemistry C*, 2019, **7**, 12306–12311.
- 17 A. M. Arevalo-Lopez, E. Solana-Madruga, C. Aguilar-Maldonado, C. Ritter, O. Mentre and J. P. Attfield, *Chem Commun (Camb)*, 2019, **55**, 14470–14473.
- 18 M. Xu, Y. Li and Y. Ma, *Chem Sci*, 2022, **13**, 329–344.
- 19 H.-K. Mao, X.-J. Chen, Y. Ding, B. Li and L. Wang, *Reviews of Modern Physics*, 2018, **90**, 015007.
- 20 M.-R. Li, J. P. Hodges, M. Retuerto, Z. Deng, P. W. Stephens, M. C. Croft, X. Deng, G. Kotliar, J. S anchez-Ben tez, D. Walker and M. Greenblatt, *Chemistry of Materials*, 2016, **28**, 3148–3158.
- 21 M.-R. Li, M. Retuerto, Z. Deng, P. W. Stephens, M. Croft, Q. Huang, H. Wu, X. Deng, G. Kotliar, J. S anchez-Ben tez, J. Hadermann, D. Walker and M. Greenblatt, *Angewandte Chemie International Edition*, 2015, **54**, 12069–12073.
- 22 C. E. Frank, E. E. McCabe, F. Orlandi, P. Manuel, X. Tan, Z. Deng, M. Croft, V. Cascos, T. Emge, H. L. Feng, S. Lapidus, C. Jin, M. Wu, M. R. Li, S. Ehrlich, S. Khalid, N. Quackenbush, S. Yu, D. Walker and M. Greenblatt, *Chem. Commun.*, 2019, **55**, 3331–3334.
- 23 A. M. Ar valo-L pez, E. Solana-Madruga, E. P. Ar valo-L pez, D. Khalyavin, M. Kepa, A. J. Dos santos Garc a, R. S ez-Puche and J. P. Attfield, *Phys. Rev. B*, 2018, **98**, 214403.
- 24 M.-R. Li, P. W. Stephens, M. Croft, Z. Deng, W. Li, C. Jin, M. Retuerto, J. P. Hodges, C. E. Frank, M. Wu, D. Walker and M. Greenblatt, *Chemistry of Materials*, 2018, **30**, 4508–4514.
- 25 S. A. Ivanov, P. Nordblad, R. Mathieu, R. Tellgren, C. Ritter, N. V. Golubko, E. D. Politova and M. Weil, *Materials Research Bulletin*, 2011, **46**, 1870–1877.
- 26 M. Numan, G. Das, M. S. Khan, G. Manna, A. Banerjee, S. Giri, G. Aquilanti and S. Majumdar, *Phys. Rev. B*, 2022, **106**, 214437.
- 27 S. A. Ivanov, R. Mathieu, P. Nordblad, R. Tellgren, C. Ritter, E. Politova, G. Kaleva, A. Mosunov, S. Stefanovich and M. Weil, *Chemistry of Materials*, 2013, **25**, 935–945.
- 28 L.  amejkal, J. Sinova and T. Jungwirth, *Physical Review X*, 2022, **12**, 031042.
- 29 J. P. Perdew, K. Burke and M. Ernzerhof, *Physical Review Letters*, 1996, **77**, 3865–3868.
- 30 P. E. Bl chl, *Physical Review B*, 1994, **50**, 17953–17979.
- 31 G. Kresse and D. Joubert, *Physical Review B*, 1999, **59**, 1758–1775.
- 32 S. L. Dudarev, G. A. Botton, S. Y. Savrasov, C. J. Humphreys and A. P. Sutton, *Physical Review B*, 1998, **57**, 1505–1509.
- 33 A. A. Coelho, *Journal of Applied Crystallography*, 2018, **51**, 210–218.
- 34 R. Mathieu, S. A. Ivanov, P. Nordblad and M. Weil, *The European Physical Journal B*, 2013, **86**, 361.
- 35 L. Zhao, Z. Hu, C.-Y. Kuo, T.-W. Pi, M.-K. Wu, L. H. Tjeng and A. C. Komarek, *physica status solidi (RRL) - Rapid Research Letters*, 2015, **9**, 730–734.
- 36 For AFM of $R\bar{3}$ the C_3 symmetry is preserved, while the S_6 symmetry in real space is combined with C_2 in spin space. The overall result is the structure still belongs to rhombohedral system.
- 37 M. Johnsson, H. Berger and R. Becker, *Acta Crystallographica Section C*, 2006, **62**, i67–i69.
- 38 W.-H. Li, C.-W. Wang, D. Hsu, C.-H. Lee, C.-M. Wu, C.-C. Chou, H.-D. Yang, Y. Zhao, S. Chang, J. W. Lynn and H. Berger, *Physical Review B*, 2012, **85**, 094431.
- 39 I. Zivkovic, K. Prsa, O. Zaharko and H. Berger, *J Phys Condens Matter*, 2010, **22**, 056002.
- 40 E. Selb, T. Buttler, O. Janka, M. Tribus, S. G. Ebbinghaus and G. Heymann, *Journal of Materials Chemistry C*, 2021, **9**, 5486–5496.
- 41 The unit cell of lattice belonging to $R3$ has two parameters a_H and c_H (or a_R and θ_R in rhombohedral representation), with volume $V_H = \frac{\sqrt{3}}{2} a_H^2 c_H$ (or $V_R = \sqrt{1 + 2\cos\theta_R}(1 - \cos\theta_R)a_R^3$). At fixed volume there is only one free parameter.
- 42 Y. Liu, S. Huang, X. Li, H. Song, J. Xu, D. Zhang and X. Wu, *Inorg Chem*, 2020, **59**, 18122–18130.
- 43 Y. Wang, J. Ying, Z. Zhou, J. Sun, T. Wen, Y. Zhou, N. Li, Q. Zhang, F. Han, Y. Xiao, P. Chow, W. Yang, V. V. Struzhkin, Y. Zhao and H. K. Mao, *Nat Commun*, 2018, **9**, 1914.
- 44 T. Kawamoto, K. Fujita, I. Yamada, T. Matoba, S. J. Kim, P. Gao, X. Pan, S. D. Findlay, C. Tassel, H. Kageyama, A. J. Studer, J. Hester, T. Irifune, H. Akamatsu and K. Tanaka, *Journal of the American Chemical Society*, 2014, **136**, 15291–15299.